Subtype-Specific Mechanisms for Functional Interaction between α6β4* Nicotinic Acetylcholine Receptors and P2X Receptors[S]

Walrati Limapichat, Dennis A. Dougherty, and Henry A. Lester

Divisions of Chemistry and Chemical Engineering (W.L., D.A.D.) and Biology and Biological Engineering (H.A.L.), California Institute of Technology, Pasadena, California

ABSTRACT

P2X receptors and nicotinic acetylcholine receptors (nAChRs) display functional and physical interactions in many cell types and heterologous expression systems, but interactions between α6β4-containing (α6β4*) nAChRs and P2X2 receptors and/or P2X3 receptors have not been fully characterized. We measured several types of crosstalk in oocytes coexpressing α6β4 nAChRs and P2X2, P2X3, or P2X2/3 receptors. A novel form of crosstalk occurs between α6β4 nAChRs and P2X2 receptors. P2X2 receptors were forced into a prolonged desensitized state upon activation by ATP through a mechanism that does not depend on the intracellular C terminus of the P2X2 receptors. Coexpression of α6β4 nAChRs with P2X3 receptors shifts the ATP dose-response relation to the right, even in the absence of acetylcholine (ACh). Moreover, currents become nonadditive when ACh and ATP are coapplied, as previously reported for other Cys-loop receptors interacting with P2X receptors, and this crosstalk is dependent on the presence of the P2X3 C-terminal domain. P2X2 receptors also functionally interact with α6β4β3 but through a different mechanism from α6β4. The interaction with P2X3 receptors is less pronounced for the α6β4β3 nAChR than the α6β4 nAChR. We also measured a functional interaction between the α6β4 nAChRs and the heteromeric P2X2/3 receptor. Experiments with the nAChR channel blocker mecamylamine on P2X2–α6β4 oocytes point to the loss of P2X2 channel activity during the crosstalk, whereas the ion channel pores of the P2X receptors were fully functional and unaltered by the receptor interaction for P2X2–α6β4β3, P2X2/3–α6β4, and P2X2/3–α6β4β3. These results may be relevant to dorsal root ganglion cells and to other neurons that coexpress these receptor subunits.

Introduction

Nicotinic acetylcholine receptors (nAChRs) and P2X receptors are ligand-gated cation channels that mediate cholinergic and purinergic fast synaptic excitation in the nervous system. The nAChRs are members of the Cys-loop receptor family, which also includes 5-HT$_3$, GABA$_{A/C}$, GluCl, and glycine receptors. Cys-loop receptors are composed of five subunits, and each subunit has four transmembrane helices and extracellular N- and C-terminal tails. There are eight neuronal α (α2–α7, α9, α10) and three neuronal β (β2–β4) nAChR subunits in mammals. nAChRs are activated by the endogenous neurotransmitter acetylcholine (ACh) as well as by nicotine. P2X receptors belong to a different family of ligand-gated cation channels and are activated by extracellular ATP. The receptors are formed by three subunits, composed of one or a combination of the seven (P2X1–P2X7) subunits. Each subunit

has two transmembrane helices and intracellular N- and C-terminal tails.

In previous work, nonindependent receptor function was demonstrated between ATP-gated channels and several members of the Cys-loop receptor family. In many cases, coactivation of P2X receptors and either α3β4 or α4β2 nicotinic, 5-HT$_{3A}$ serotonin, or GABA$_{A/C}$ receptors leads to cross-inhibitory interactions revealed by nonadditivity of the recorded currents (Searl et al., 1998; Zhou and Galligan, 1998; Khakh et al., 2000, 2005; Boué-Grabot et al., 2003, 2004a,b; Xia et al., 2008; Decker and Galligan, 2010). Cys-loop receptors and P2X receptors are coexpressed at many postsynaptic membranes, and ATP is coreleased with other fast neurotransmitters at presynaptic terminals (Silinsky and Hubbard, 1973; Silinsky, 1975). Therefore, the interactions between their respective receptor channels may play a critical role in shaping synaptic currents.

There is evidence that the crosstalk between the P2X and the Cys-loop families of ligand-gated ion channels involves physical interaction between the ion channel proteins during simultaneous agonist application. The proposed models commonly entail a general mechanism of state-dependent "conformational spread," or propagation of allosteric states in

---

ABBREVIATIONS: α6β4*, a pentameric nicotinic acetylcholine receptor containing at least one α6 subunit, at least one β4 subunit, and other subunits to be specified; αβmeATP, α,β-methylene-ATP; ACh, acetylcholine; DRG, dorsal root ganglion; Mec, mecamylamine; nAChR, nicotinic acetylcholine receptor.

large multiprotein complexes, from one receptor to the other (Khakh et al., 2000, 2005; Bray and Duke, 2004). Through this conformational spread, the motion triggered by the gating of one channel type is communicated to the other channels and induces their closure. A prerequisite for such a mechanism is the close proximity of receptors. Previous work confirmed physical interactions for combinations of P2X2–$\alpha 4\beta 2$, P2X2–5-HT$_3$, and P2X2–GABA$_C$ receptors (Khakh et al., 2000, 2005; Boué-Grabot et al., 2003, 2004a,b; Toulmé et al., 2007; Decker and Galligan, 2010; Jo et al., 2011; Shrivastava et al., 2011). The evidence for physical contact suggests that there is no major role for second messengers generated by endogenous and electrophysiologically silent metabotropic P2Y receptors in the cross inhibition.

Dorsal root ganglion (DRG) neurons express $\alpha 6\beta 4^*$ nAChR and P2X2, P2X3, and P2X2/3 receptors (Cockayne et al., 2000, 2005; Souslova et al., 2000; Hone et al., 2011; Beggs et al., 2012). Studies with recombinant nAChRs have identified two subunit combinations of $\alpha 6\beta 4^*$ nAChRs: $\alpha 6\beta 4$ and $\alpha 6\beta 4\beta 3$ (Grinevich et al., 2005; Tumkosit et al., 2006; Dash and Lukas, 2012; Jensen et al., 2013). $\beta 3$ coassembles with $\alpha 6$ into nicotinic receptor pentamers at several locations in the brain but does not participate in forming the $\alpha/$non-α interface that comprises the neuronal ligand-binding site. Therefore, other β subunits, either $\beta 2$ or $\beta 4$, must be present to form functional nicotinic receptors with $\alpha 6$ and $\beta 3$. Förster resonance energy transfer has demonstrated physical interactions between P2X2 or P2X3 receptors and $\alpha 6\beta 4$ receptors in Neuro2a cells and cultured mouse cortical neurons, and the incorporation of $\beta 3$ did not show any effect on the binding fraction or the energy transfer efficiency (unpublished data).

In this study, we detected and analyzed the mechanism of a functional interaction between $\alpha 6\beta 4^*$ nAChRs and three P2X receptors (homomeric P2X2, homomeric P2X3, and heteromeric P2X2/3 receptors) in *Xenopus laevis* oocytes. We find two distinct types of interaction. One is inhibitory and occurs only during receptor coactivation by both ACh and ATP, consistent with the conformational spread hypothesis. The other type of interaction is preorganized and constitutive, in which a biophysical property of one channel is modulated by the other. Our results have elucidated detailed features of P2X–$\alpha 6\beta 4$ functional crosstalk, and highlight, for the first time, the distinct mechanisms of interaction between specific receptor subtypes.

Materials and Methods

Molecular Biology. Rat $\alpha 6$ and mouse $\beta 3$ nAChRs were in the pGEMhe vector, and rat $\beta 4$ nAChR was in the pAMV vector. All P2X cDNAs were in the pcDNA3 vector. Site-directed mutagenesis was performed using the Stratagene QuikChange protocol. Truncated P2X2 and P2X3(K65A) subunits were made by engineering a TAA stop codon at the 3' end of the sequence encoding the residue 373 of P2X2 or residue 385 of P2X3(K65A). Circular cDNA was linearized with NheI (for the pGEMhe vector), NotI (for the pAMV vector), or XhoI (for the pcDNA3 vector). After purification (Qiagen, Valencia, CA), linearized DNA was used as a template for runoff in vitro transcription using a T7 mMessage mMachine kit (Ambion, Austin, TX). The resulting mRNA was purified (RNAeasy Mini Kit; Qiagen) and quantified by UV spectroscopy.

Expression of $\alpha 6\beta 4^*$ nAChRs and P2X Receptors in *Xenopus* Oocytes. *X. laevis* oocytes (stage V to VI) were utilized. Each oocyte was injected with 50 nl mRNA solution. When $\alpha 6\beta 4^*$ nAChRs and

P2X receptors are coexpressed, equal volumes of corresponding mRNA solutions were mixed prior to the oocyte injection. To express the $\alpha 6\beta 4$ combination, we used the hypersensitive $\alpha 6$ subunit containing a serine mutation at the leucine 9' on M2 (residue 279). The mRNA ratio used was 2:5 $\alpha 6$(L9'S):$\beta 4$ by mass, and we injected 25–50 ng total mRNA per cell. We used the wild-type $\alpha 6$ and $\beta 4$ in combination with the hypersensitive $\beta 3$ containing a serine mutation at the valine 13' on M2 (residue 283) to express the $\alpha 6\beta 4\beta 3$ combination. The wild-type $\alpha 6\beta 4$ produced no detectable current signal, with or without coinjection of the P2X subunits. Cells were injected with a mixture of mRNA at the ratio of 2:2:5 $\alpha 6$:$\beta 4$:$\beta 3$(V13'S) at a total mRNA concentration of 5–20 ng per cell. The optimal mRNA concentration of P2X2 was 0.05 ng per cell when expressed alone and 0.1–0.3 ng per cell when coexpressed with $\alpha 6\beta 4^*$ nAChR. To study P2X3, we used the K65A mutation, which enhanced the rate of recovery from desensitization. We injected 5 ng P2X3(K65A) mRNA per cell when expressed alone and 10–20 ng mRNA when coexpressed with $\alpha 6\beta 4^*$ nAChR. P2X2/3 was expressed by coinjection of a 1:10 ratio of P2X2:P2X3 mRNA at 15–25 ng total mRNA. To express P2X2(T18A) and the truncated P2X subunits, 25–50 ng mRNA per cell was required. After mRNA injection, cells were incubated for 24–72 hours at 18°C in culture medium (ND96$^+$ with 5% horse serum).

Electrophysiology. ACh chloride was purchased from Sigma-Aldrich/RBI (St. Louis, MO) and stored as 1-M stock solutions. ATP and α,β-methylene-ATP ($\alpha\beta$meATP) were purchased from Tocris Bioscience (Bristol, UK) and were stored as 100-mM stock solutions. Mecamylamine (Mec) hydrochloride was purchased from Sigma-Aldrich/RBI and stored as 100-mM stock solutions. All stock solutions were stored at -80°C, and drug dilutions were prepared from the stock solution in Ca^{2+}-free ND96 buffer within 24 hours prior to the electrophysiological recordings. The pH of all buffers and drug solutions was adjusted to 7.4.

Agonist-induced currents were assayed in two-electrode voltage-clamp mode using the OpusXpress 6000A (Axon Instruments, Sunnyvale, CA). Up to eight oocytes were simultaneously voltage clamped at -60 mV. All data were sampled at 125 Hz and filtered at 50 Hz.

For P2X2, $\alpha 6$(L9'S)$\beta 4$, or $\alpha 6\beta 4\beta 3$(V13'S) dose-response experiments, 1 ml total agonist solution was applied to cells, and 7 to 8 concentrations of agonist were used. Mixtures of ATP and ACh were prepared beforehand in cases of agonist coapplication. Cells were perfused in Ca^{2+}-free ND96 solution before agonist application for 30 seconds, followed by a 15-second agonist application and a 2-minute wash in Ca^{2+}-free ND96 buffer. A similar protocol was used to investigate cross interaction between P2X2 and $\alpha 6\beta 4^*$, except that the wash was extended to 3 minutes. We used 100 μM ACh and 1 mM ATP in all cross interaction experiments. The order of application was ACh, ATP, and ACh + ATP, unless otherwise specified. We used 50 μM and 500 μM Mec to block $\alpha 6\beta 4\beta 3$(V13'S) and $\alpha 6$(L9'S)$\beta 4$ receptors, respectively. In all experiments involving Mec, oocytes were incubated with 0.25 ml Mec (or buffer) for approximately 20 seconds prior to an application of a premixed solution of agonist and Mec (or just agonist). The order of application was ACh, ATP, ACh + ATP, and ACh + ATP + Mec.

To ensure robust currents, we only analyze data from cells that produced between 5 and 13 μA of ATP-evoked current (I_{ATP}) and >1.5 μA of ACh-evoked current (I_{ACh}). Cells displaying larger currents were discarded to avoid series resistance artifacts as well as pore dilation, a phenomenon known to occur for P2X2 receptors at high receptor density (Eickhorst et al., 2002; Fujiwara and Kubo, 2004; Vial et al., 2004; Egan et al., 2006; Jarvis and Khakh, 2009).

For ATP dose-response experiments on the fast-desensitizing (<1 second) P2X receptors, including P2X3, P2X3(K65A), and P2X2(T18A) receptors and P2X3 truncated receptors (P2X3TRs), ATP application was 2 seconds in duration at the total volume of 0.5 ml, and the wash was 3.5 minutes. For ATP dose-response experiments in the presence of ACh, ACh was preapplied for 15 seconds through pump B (0.6 ml), followed by a 2-second application of a mixture of ATP and ACh

(0.5 ml), another 30 seconds of ACh application through pump B (1.5 ml), and a 164-second wash in Ca^{2+}-free ND96. Cross interaction between these fast-desensitizing P2X receptors and $\alpha6\beta4^*$ nAChRs was probed in an experiment that involved an alternate application of saturating ATP doses without ACh and with ACh, using the same protocol as the dose-response experiments, except that the wash time used was 164-second in duration. The concentration of ACh was 100 μM in all cross interaction experiments, and the concentrations of ATP were 100 μM for cells expressing P2X3(K65A) and $\alpha6\beta4\beta3$ (V13′S), 320 μM for P2X3(K65A) and $\alpha6$(L9′S)$\beta4$, 320 μM for P2X3TR and $\alpha6$(L9′S)$\beta4$, and 1 mM for P2X2(T18A) and $\alpha6$(L9′S)$\beta4$. Peak currents from at least three traces were averaged from the same cell for data analysis. Data from cells displaying <1.5 μA of I_{ACh}, <5 μA or >11 μA of I_{ATP}, or $I_{ACh} > I_{ATP}$ were excluded from all cross interaction analysis.

To investigate cross interaction between the P2X2/3 receptor and $\alpha6\beta4^*$ nAChR, the P2X2/3 receptor was activated by 100 μM $\alpha\beta$meATP, and $\alpha6\beta4^*$ nAChR by 100 μM ACh. All agonist applications were 10 seconds in duration at a volume of 0.5 ml, followed by an additional 5 seconds of incubation with the agonist(s) without fluid aspiration. The cells were then washed for approximately 5 minutes. The order of application was $\alpha\beta$meATP, ACh, and $\alpha\beta$meATP + ACh, unless specified otherwise. A similar protocol was used for experiments with Mec, and in addition, cells were preincubated in 0.25 ml of either buffer or Mec solution prior to the application of the test doses, in the same manner as described above for P2X2–$\alpha6\beta4^*$. We used 50 μM and 500 μM Mec to block $\alpha6\beta4\beta3$(V13′S) and $\alpha6$(L9′S)$\beta4$ receptors, respectively. Only data from cells displaying $I_{\alpha\beta meATP}$ between 5 and 13 μA, $I_{ACh} \geq 1.5$ μA, and $I_{\alpha\beta meATP} > I_{ACh}$ were included in the analysis.

Data Analysis. All dose-response data were normalized to the maximal current ($I_{max} = 1$) of the same cell and then averaged. The EC_{50} and Hill coefficient (n_H) were determined by fitting averaged, normalized dose-response relations to the Hill equation. Dose responses of individual oocytes were also examined and used to determine outliers.

For all cross interaction data involving P2X2 or P2X2/3, including data from the Mec experiments, the predicted current from agonist coapplication was calculated from the arithmetic sum of I_{ACh} and I_{ATP} (or $I_{\alpha\beta meATP}$) from the same cell. The actual, observed current upon coapplication of the agonists was subtracted from the prediction value of the same cell, and this difference was designated as Δ. All current data and Δ were normalized to the prediction value of the same cell, and then the normalized data were averaged across at least seven cells from at least two batches of oocytes.

We utilized the "prolonged plus brief pulse" protocol (Fig. 4) for all cross interaction data involving the fast-desensitizing P2X receptors, including P2X3, P2X3(K65A), P2X3TR, and P2X2(T18A) receptors, averaged ATP-evoked peak current during ACh application (I_{ATP}^*) was subtracted from averaged ATP-evoked current in the absence of ACh (I_{ATP}) from the same cell to obtain a Δ^*. All current data and Δ^* were normalized to (I_{ATP}) and averaged across at least eight cells from at least two batches of oocytes.

All data are presented as the mean ± S.E.M., with statistical significance assessed by the paired t test. A P value of <0.01 was accepted as indicative of a statistically significant difference.

Results

Functional Interaction between $\alpha6\beta4$ and Homomeric P2X2 Receptors. Previous work reported that most $\alpha6$-containing nAChRs expressed in heterologous systems produced very small agonist-induced currents, making accurate measurements impossible. We measured similarly small currents for both $\alpha6\beta4$ and $\alpha6\beta2$ subtypes with human, rat, and mouse $\alpha6$ subunits expressed in *Xenopus* oocytes. We confirmed that the problem could be overcome by introducing a gain-of-function mutation in the $\alpha6$ subunit, $\alpha6$(L9′S) (Drenan et al., 2008a; Dash and Lukas, 2012), in studies of $\alpha6\beta4$ receptors. All studies described here using $\alpha6\beta4$ utilize this mutation, and we omit the L9′S notation for simplicity. Although obtaining sufficient $\alpha6\beta4$ currents from *X. oocytes* was challenging, the expression of P2X2 receptors was very robust, frequently producing currents >20 μA.

When we coexpressed P2X2 with $\alpha6\beta4$ in oocytes, we observed both ACh-evoked current (I_{ACh}) and ATP-evoked current (I_{ATP}) from the same cell. We found only minor (<2-fold) changes in the EC_{50} values for both ACh and ATP when P2X2 and $\alpha6\beta4$ are coexpressed (Supplemental Table 1). Furthermore, coapplication of ACh and ATP had only a weak effect with respect to the dose-response relation of the individual agonist.

We probed the interaction between the P2X2 and $\alpha6\beta4$ receptors by applying the agonists simultaneously, paralleling previous work that investigated functional interactions between P2X2 and other Cys-loop receptors. The resulting peak current observed during the coapplication of ACh and ATP ($I_{ACh+ATP}$) was compared with the arithmetic sum of the individual ACh- and ATP-induced currents at the same agonist concentrations on the same cell. If the two families of receptors are functionally independent (i.e., if there is no interaction between them), $I_{ACh+ATP}$ is expected to equal the sum of I_{ACh} and I_{ATP} of the same cell.

Initially, the agonists were applied in the following sequence: 100 μM ACh, 1 mM ATP, and then coapplication of 100 μM ACh and 1 mM ATP (Fig. 1A). In oocytes coexpressing P2X2–$\alpha6\beta4$, we found that when 100 μM ACh and 1 mM ATP were applied simultaneously, the total current was approximately 20% less than the sum of the currents elicited by the individual agonist at the same concentrations (Fig. 1), which is the conventional definition of "cross inhibition." The difference between the predicted current and the observed $I_{ACh+ATP}$ is denoted as Δ. In most cells, $I_{ACh+ATP}$ was only slightly larger than I_{ATP}, reported as mean normalized current in Fig. 1B, and consequently, Δ was nearly the size of I_{ACh}. When the analogous experiments were performed on cells expressing only $\alpha6\beta4$ or only P2X2, we found that ATP did not activate or modulate the $\alpha6\beta4$ nAChRs, and ACh did not activate or modulate the P2X2 receptors (Supplemental Fig. 1A). The cross inhibition observed during coapplication of ACh and ATP at saturating doses suggests that P2X2 and $\alpha6\beta4$ receptors are functionally dependent when coexpressed.

Effect of Order of Agonist Application on P2X2–$\alpha6\beta4$ Cross Inhibition. Interestingly, when we applied agonists in the order of ACh, ATP, (ACh + ATP), ATP, and ACh to P2X2–$\alpha6\beta4$ oocytes, we consistently found that the current evoked by the second ATP application is smaller than the first one (Supplemental Fig. 2). By contrast, a similar current reduction was never observed for ACh. This suggested that the order of agonist application could impact the observed cross-inhibitory behavior. As such, we varied the order of agonist applications in six different combinations. We observed cross inhibition in three of six cases (Fig. 2, A–C), all of which involved the application of ATP before the mixture of ACh and ATP. In the other three cases (Fig. 2, D–F) in which ACh + ATP was applied before ATP, we observed current additivity—$I_{ACh+ATP}$ was comparable to the sum of I_{ACh} and I_{ATP}. This phenomenon was unique to the P2X2–$\alpha6\beta4$ interacting pair; it was not seen for the other receptor combinations studied herein.
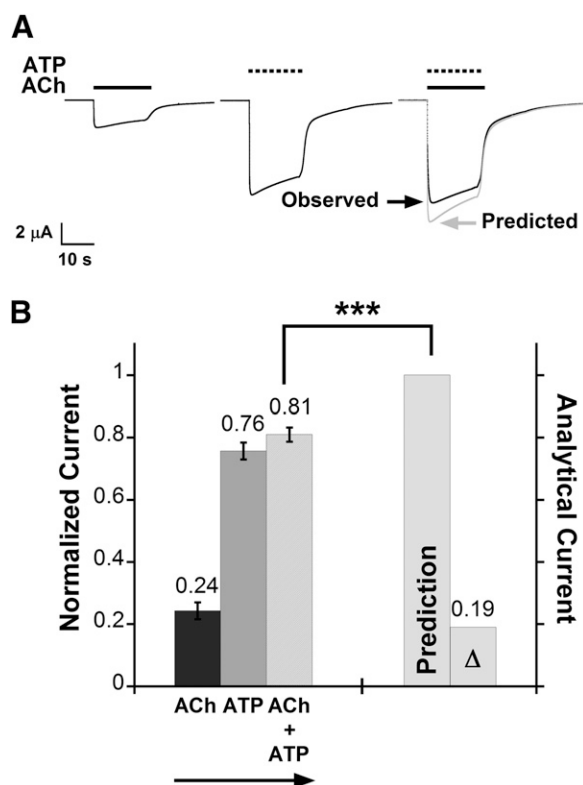
Fig. 1. Functional interaction between the $\alpha6\beta4$ nAChR and the homomeric P2X2 receptor. (A) Representative current traces (black) from one oocyte coexpressing $\alpha6\beta4$ and P2X2 receptors during application of ACh (100 μM), ATP (1 mM), or the ACh + ATP mixture. The predicted waveform is the point-by-point arithmetic sum of the I_{ACh} and I_{ATP} waveforms (gray). P2X2–$\alpha6\beta4$ oocytes displayed cross inhibition: The current evoked by coapplication of ACh and ATP is smaller than the prediction. (B) Mean normalized currents $\pm$ S.E.M. are shown for current signals measured from P2X2–$\alpha6\beta4$ oocytes (n = 16 cells) upon receptor activation by ACh (100 μM), ATP (1 mM), or ACh + ATP. The arrow indicates sequence of agonist application. Mean current amplitudes $\pm$ S.E.M. for ACh, ATP, and ACh + ATP are 2.91 $\pm$ 0.34 μA, 9.48 $\pm$ 0.83 μA, and 10.07 $\pm$ 0.76 μA, respectively. All measured agonist-induced currents were normalized to the predicted arithmetic sum of ACh- and ATP-induced current ("Prediction" column) of the same cell and then averaged. Δ is the mean difference between the prediction and the observed $I_{ACh+ATP}$. The paired t test was performed to compare un-normalized $I_{ACh+ATP}$ data to the predicted values. $I_{ACh+ATP}$ is smaller than the predicted values, consistent with functional interaction between $\alpha6\beta4$ and P2X2 receptors. ***$P < 0.0005$.

Recovery from Desensitized State of P2X2 in the Presence of $\alpha6\beta4$ Receptor. A possible interpretation for the results in Fig. 2 is that we did not allow enough time for P2X2 to recover from its desensitized state. This is not the case for oocytes expressing P2X2 alone, because application of ACh → ATP → (ACh + ATP), respectively, produced no ACh-evoked current and identical current amplitudes for ATP and ATP + ACh (Supplemental Fig. 1A). However, the functional interaction between $\alpha6\beta4$ and P2X2 may alter the P2X2 desensitization behavior from the isolated P2X2 receptor. Supporting this hypothesis, oocytes expressing both P2X2 and $\alpha6\beta4$ typically produced ATP-evoked current traces with noticeable desensitization, unlike oocytes expressing P2X2 alone (Supplemental Fig. 3). As such, we asked whether the interaction with the $\alpha6\beta4$ nAChR had any effect on the lifetime of the P2X2 desensitized state. Peak ATP-evoked current (I_{ATP}) was recorded while consecutive doses of 1 mM ATP were applied, with a 3-minute interval between doses, on
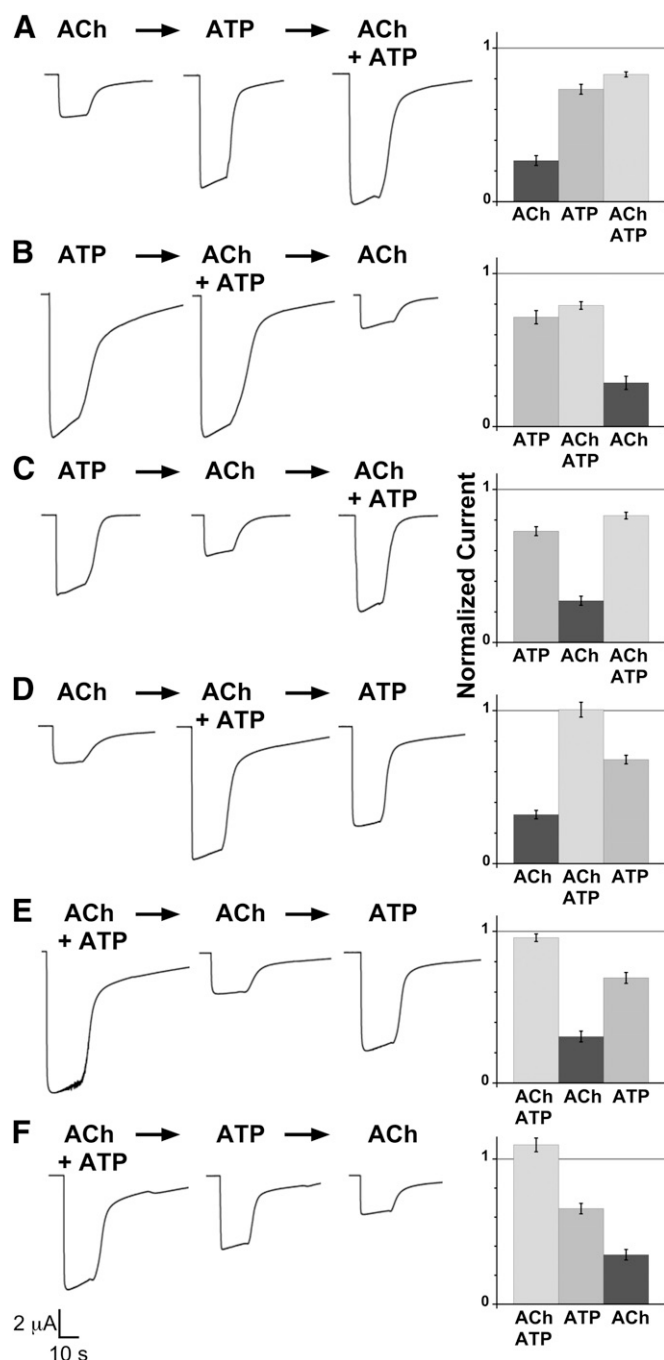

Fig. 2. The sequence of agonist applications determines cross inhibition in $\alpha6\beta4$–P2X2 oocytes. (A–F) The left images show representative current traces from an oocyte coexpressed with $\alpha6\beta4$ and P2X2 receptors upon application of ACh (100 μM), ATP (1 mM), or ACh + ATP from left to right sequentially. The scale bar is applied for all traces. The right graphs show mean normalized currents $\pm$ S.E.M. for agonist-induced currents measured from P2X2–$\alpha6\beta4$ oocytes (n = 7, 9, 9, 9, 7, and 10 for A–F, respectively). All measured current signals were normalized to the predicted arithmetic sum of ACh- and ATP-induced current of the same cell, shown as the horizontal line as reference, and then averaged. Coapplication of ACh and ATP produced either nonadditive current (A–C) or additive current (D–F), depending on the sequence of agonist application. Mean current amplitudes $\pm$ S.E.M. are as follows: 2.71 $\pm$ 0.37 μA for ACh, 7.74 $\pm$ 1.14 μA for ATP, and 8.65 $\pm$ 1.09 μA for ACh + ATP (A); 6.98 $\pm$ 1.20 μA for ATP, 7.41 $\pm$ 0.96 μA for ACh + ATP, and 2.40 $\pm$ 0.28 μA for ACh (B); 8.02 $\pm$ 1.17 μA for ATP, 2.68 $\pm$ 0.12 μA for ACh, and 8.99 $\pm$ 1.15 μA for ACh + ATP (C); 2.65 $\pm$ 0.27 μA for ACh, 9.51 $\pm$ 1.64 μA for ACh + ATP, and 6.42 $\pm$ 1.13 μA for ATP (D); 9.28 $\pm$ 1.16 μA for ACh + ATP, 3.01 $\pm$ 0.50 μA for ACh, and 6.70 $\pm$ 0.82 μA for ATP (E); and 9.11 $\pm$ 0.86 μA for ACh + ATP, 5.86 $\pm$ 0.95 μA for ATP, and 2.71 $\pm$ 0.25 μA for ACh (F).

either oocytes expressing P2X2 alone or oocytes expressing P2X2–α6β4. The P2X2 oocytes showed normal recovery of current signal (Fig. 3A). However, we observed a meaningful reduction in current size from the P2X2–α6β4 oocytes upon repeating applications of 1 mM ATP (Fig. 3B). It is important to note that in these experiments, cells had never been pre-exposed to an agonist (i.e., the oocytes were naïve). Similar loss of ATP-evoked current was observed when the P2X2–α6β4 oocytes were preexposed to ACh (Fig. 3C). The original ATP current level could be recovered after >10 minutes of wash in buffer solution (data not shown), which suggests that the current reduction was due to a slow recovery from the desensitized state. When P2X2–α6β4 oocytes were preexposed to a mixture of ACh and ATP, repeating ATP doses caused no reduction in current amplitude (Fig. 3D), which implicates that the subpopulation of P2X2 has already been desensitized after the coapplication of ACh and ATP.

We then asked whether desensitized P2X2 receptors would functionally interact with α6β4 nAChR. We applied a series of agonists to the P2X2–α6β4 oocytes as follows: ACh, four repeating doses of 1 mM ATP, and ACh + ATP. As expected, ATP-evoked current was smaller upon repeating ATP doses (Fig. 3E, first through fourth ATP), consistent with a subpopulation of P2X2 being desensitized. Ultimately, no cross inhibition was seen—$I_{ACh+ATP}$ was within the error of the predicted sum of the ACh current and the fourth ATP current (Fig. 3E). The data demonstrate that the desensitized P2X2 did not functionally interact with the α6β4 nAChR; therefore, P2X2 desensitization alone can fully explain the cross-inhibitory behavior observed for P2X2–α6β4 interaction.

Functional Interaction between α6β4 and Homomeric P2X3 Receptors. In *Xenopus* oocytes, P2X3 receptors produced sizeable currents (>1 μA) that desensitize very rapidly (probable time constant <1 second) and require >30 minutes to recover fully from the desensitized state. The K65A mutation, near the ATP the binding site, slightly reduces the rate of desensitization and moderately enhances the rate of current recovery for the P2X3 receptor (Pratt et al., 2005). We have included this mutation in all studies involving the homotrimeric P2X3 receptor, and again, we leave out the K65A notation for simplicity.

Unlike P2X2, the fast-desensitization kinetics of the P2X3 channels did not allow us to probe the functional interaction with α6β4 by simultaneous application of ACh and ATP. Instead, ATP-evoked current when a 2-second pulse of ATP was applied alone (I_{ATP}) was compared with the current evoked by the ATP pulses superimposed on a prolonged 47-second application of ACh that was begun before ATP (I_{ATP*}) (Fig. 4A, inset). We term this procedure the "prolonged plus brief pulse" protocol. The difference between I_{ATP} and I_{ATP*} (Δ*) would directly indicate cross interaction between the two receptors. To validate the prolonged plus brief pulses protocol, we used the mutation T18A in P2X2; this mutant drastically increases the rate of receptor desensitization, rendering the waveforms comparable to the P2X3 responses. We verified that the P2X2-T18A mutant produced an ATP dose-response relation resembling the wild-type P2X2 receptor and also displayed cross inhibition with α6β4 (Supplemental Fig. 4).

Both ACh- and ATP-evoked currents were observed in oocytes coexpressing α6β4 and P2X3 receptors. At 100 μM ACh and 320 μM ATP, P2X3–α6β4 oocytes displayed cross inhibition in that I_{ATP} was smaller than I_{ATP*} by 20% (Fig. 4A). Control experiments on cells injected with only P2X3 mRNA confirmed that ACh did not activate or modulate P2X3 receptors (Supplemental Fig. 1B). However, ACh-evoked current when ACh was applied after ATP (without wash) was comparable to ACh-evoked current when ACh was applied alone in the absence of ATP (data not shown), indicating that the cross inhibition does not occur when P2X3 receptors are already desensitized.
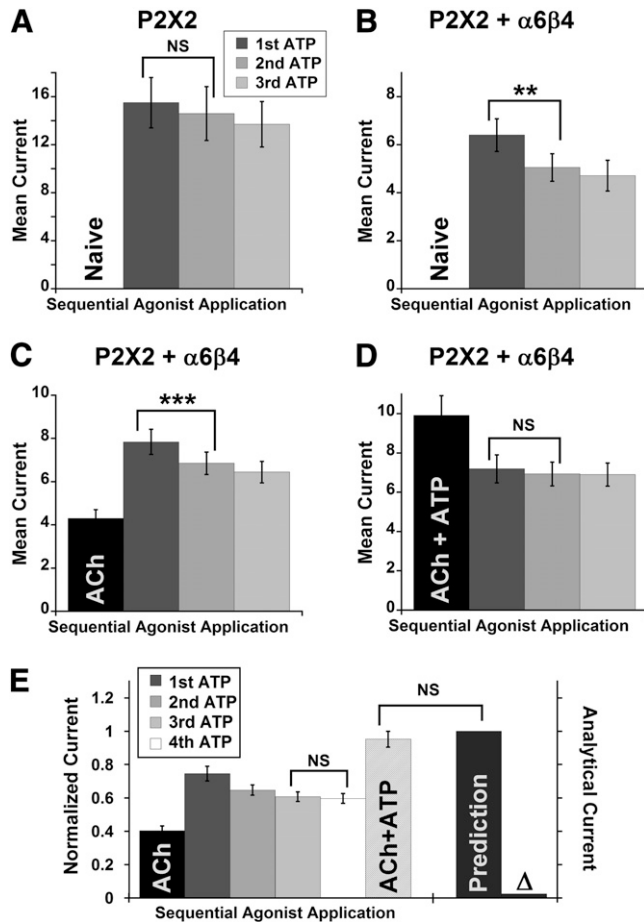

Fig. 3. The presence of α6β4 hindered recovery from a desensitized state of the P2X2 channel, and cross inhibition was not observed between desensitized P2X2 and α6β4. (A–D) Mean current amplitudes from three consecutive doses of 1 mM ATP applied to P2X2 oocytes (A) or P2X2–α6β4 oocytes (B–D) with a 3-minute wash interval between doses, with or without prior exposure to ACh (n = 8, 7, 12, and 13 for A–D, respectively). ATP-evoked current from P2X2 oocytes display a normal, nearly complete recovery from desensitization (A), whereas the current from naïve P2X2–α6β4 oocytes recovered only partially after the first ATP dose (B). Incomplete recovery of current was also observed from oocytes that were exposed to ACh (100 μM) prior to the consecutive doses of ATP (C). When oocytes were preexposed to an ACh + ATP mixture, however, no reduction in current amplitudes was observed upon repeating application of ATP alone (D). (E) P2X2–α6β4 oocytes were exposed to 100 μM ACh, 4 × 1 mM ATP, and (100 μM ACh + 1 mM ATP), respectively, with a 3-minute wash interval between agonist applications. Currents were normalized to the prediction from the individual cell (I_{ACh} + fourth I_{ATP}), and then averaged (n = 13). Δ is the difference between the prediction and the observed $I_{ACh+ATP}$. There is no significant difference between the observed $I_{ACh+ATP}$ and prediction, with Δ is approximately equal to 0, suggesting desensitized P2X2 did not functionally interact with α6β4. Mean current amplitudes ± S.E.M. are as follows: 4.30 ± 0.40 μA for ACh, 7.84 ± 0.58 μA for first ATP, 6.85 ± 0.52 μA for second ATP, 6.44 ± 0.50 μA for third ATP, 6.34 ± 0.52 μA for fourth ATP, and 10.17 ± 0.81 μA for ACh + ATP. The averaged Δ before normalization is 0.47 ± 0.25 μA. **$P < 0.005$; ***$P < 0.0005$. NS, not significant ($P \geq 0.05$).
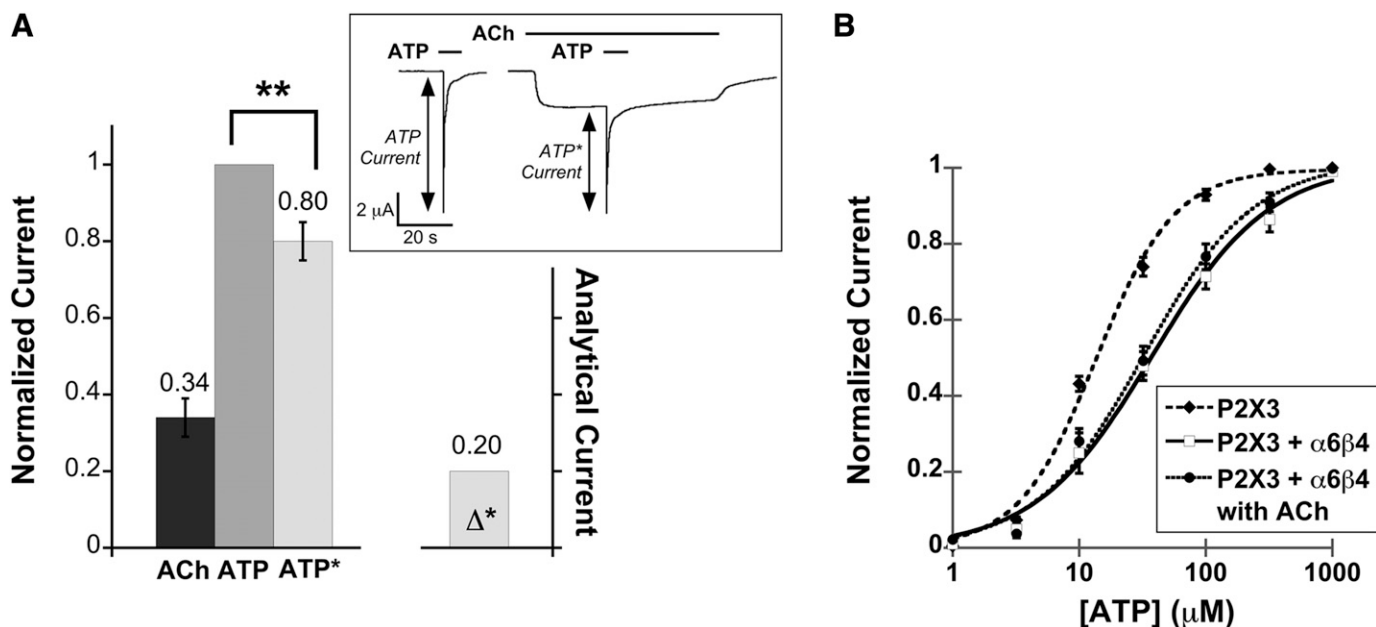
A

B

Fig. 4. Functional interaction between the $\alpha6\beta4$ nAChR and the homomeric P2X3 receptor. (A) Mean, normalized current $\pm$ S.E.M. is shown for the peak of agonist-induced currents measured from P2X3–$\alpha6\beta4$ oocytes ($n = 12$) upon application of ACh (100 μM), ATP (100 μM), and ATP with ACh preapplication (ATP*). Mean current amplitudes $\pm$ S.E.M. are 2.57 $\pm$ 0.50 μA for ACh, 7.29 $\pm$ 0.65 μA for ATP, and 6.4 $\pm$ 0.75 μA for ATP*. All measurements were normalized to the ATP current of the same cell and then averaged. $\Delta*$ is the mean difference between I_{ATP} and I_{ATP*}. **$P < 0.005$. The insert shows the protocol used for probing cross inhibition between the $\alpha6\beta4$ nAChR and the fast-desensitizing P2X receptor. ATP was applied alone or after a preapplication of ACh. For both I_{ATP} and I_{ATP*}, at least three agonist-induced currents were averaged from the same cell. The resulting I_{ATP} and I_{ATP*} currents were then compared with determine cross inhibition. (B) ATP dose-response curves for P2X3 oocytes (EC$_{50}$ 13.6 $\pm$ 1.3 μM, Hill constant 1.4 $\pm$ 0.16, $n = 12$), P2X3–$\alpha6\beta4$ oocytes in the absence of ACh (EC$_{50}$ 37.8 $\pm$ 6.1 μM, Hill constant 0.94 $\pm$ 0.11, $n = 14$), and P2X3–$\alpha6\beta4$ oocytes in the presence of 100 μM ACh (EC$_{50}$ 32.8 $\pm$ 5.0 μM, Hill constant 1.0 $\pm$ 0.12, $n = 11$). The fitted curves show that the P2X3 cells were less sensitive to ATP when $\alpha6\beta4$ was coexpressed, regardless of nAChR activation by ACh.

In addition, we found that the ATP dose-response curve was shifted rightward in oocytes coexpressing $\alpha6\beta4$ and P2X3 compared with the oocytes expressing P2X3 alone. The EC$_{50}$ of the P2X3 receptor is approximately 3-fold higher and the Hill coefficient is reduced (Fig. 4B), suggesting a decrease in cooperativity. Conversely, coexpression of the two receptors did not affect the ACh EC$_{50}$ relative to oocytes expressing only $\alpha6\beta4$ nAChR. Note that the EC$_{50}$ values for ATP and ATP* are essentially identical (Supplemental Table 1). This means that the shift in ATP EC$_{50}$ in the presence of $\alpha6\beta4$ is independent of ACh.

Roles of P2X C-Terminal Domain in P2X–$\alpha6\beta4$ Functional Interaction. The C-terminal domains of P2X2 and P2X3 were previously shown to be crucial for their functional interaction with the 5-HT$_{3A}$ receptor, the $\alpha4\beta3$ nAChR, and the GABA$_C$ receptor. Here we sought to investigate the importance of the C termini of both P2X2 and P2X3 in the interaction with $\alpha6\beta4$ nAChRs. We removed the C-terminal tails from both P2X2 and P2X3(K65A) constructs and denoted the resulting truncated receptors as P2X2TR and P2X3TR, respectively.

In $\alpha6\beta4$–P2X2TR oocytes, the results were similar to what was seen with the full-length P2X2 receptor. We observed mean $I_{ACh+ATP}$ values that were 20% smaller than the predicted values when the agonists were applied in the following sequence: ACh $\rightarrow$ ATP $\rightarrow$ ACh + ATP (Fig. 5A). When we switched the order of agonist application to ACh + ATP $\rightarrow$ ATP $\rightarrow$ ACh, no cross inhibition was observed (Fig. 5B). Therefore, the C-terminal tail of P2X2 is not required for the functional interaction between the P2X2 receptor and the $\alpha6\beta4$ nAChRs.

The P2X3TR receptors had a comparable ATP EC$_{50}$ to the full-length P2X3 receptors. Parallel to what was seen with the full-length receptors, coexpression with $\alpha6\beta4$ shifted the ATP dose-response curve to the right, increasing the ATP EC$_{50}$ (Fig. 5C). However, we did not observe any meaningful cross inhibition between P2X3TR and $\alpha6\beta4$ at a saturating ATP concentration (320 μM) (Fig. 5D). These results suggest that the C-terminal domain of P2X3 is crucial for current cross inhibition at saturating ACh and ATP concentrations but is not involved in shifting the ATP EC$_{50}$ for the interacting P2X3–$\alpha6\beta4$ receptors.

Functional Interaction between $\alpha6\beta4$ and Heteromeric P2X2/3 Receptors. We expressed the heteromeric P2X2/3 receptor by coinjecting oocytes with both wild-type P2X2 and wild-type P2X3 mRNA, which is reported to produce the heteromeric P2X2/3 receptor, along with the homomeric P2X2 and P2X3 receptors. To isolate the P2X2/3 current, we used the agonist $\alpha\beta$meATP, an ATP analog known to selectively activate the P2X3 and P2X2/3 receptor populations. Oocytes expressing P2X2 produced no current upon $\alpha\beta$meATP application. In oocytes expressing the P2X2/3 receptor, $\alpha\beta$meATP-evoked current traces were clearly distinct from what was seen from P2X3 oocytes, displaying slower apparent desensitization kinetics (Supplemental Fig. 5A). Since the wild-type P2X3 receptor desensitizes very rapidly, we can define signals that correspond exclusively to P2X2/3 receptors. Furthermore, the mRNA injection ratio (P2X2:P2X3 = 1:10 by mass) was optimized such that any current from the homomeric P2X3 receptor was negligible at the saturating dose of $\alpha\beta$meATP.

Desensitization of P2X2/3 current was slow enough to allow investigation of the functional interaction with $\alpha6\beta4$ by
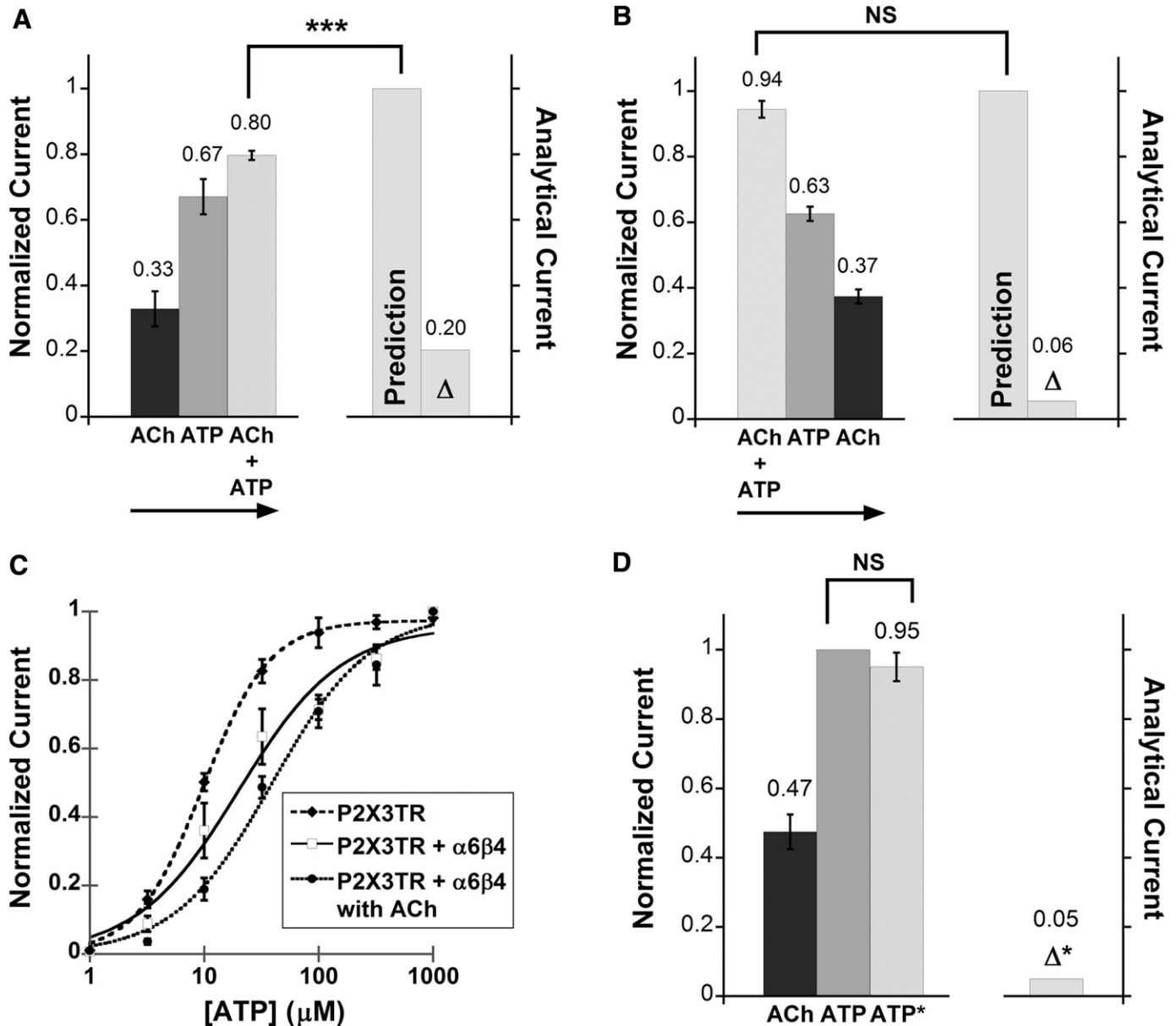
Fig. 5. Functional interaction between α6β4 and C-terminally truncated P2X receptors. (A and B) P2X2TR behaves like the full-length P2X2 with respect to the functional interaction with α6β4 receptor. Namely, application of ATP before the ACh +ATP mixture resulted in current cross inhibition, but current additivity was observed when ACh +ATP was applied before ATP. Mean normalized currents ± S.E.M. are shown for current signals measured from P2X2TR–α6β4 oocytes (n = 8 and 11 for A and B, respectively) upon receptor activation by of ACh, ATP, or ACh + ATP. The arrows indicate sequential agonist application. (A) Mean current amplitudes ± S.E.M. are 3.75 ± 0.83 μA, 6.90 ± 0.83 μA, and 8.53 ± 0.94 μA for ACh, ATP, and ACh + ATP, respectively. (B) Mean current amplitudes ± S.E.M. are 14.52 ± 1.28 μA, 9.67 ± 0.90 μA, and 5.64 ± 0.51 μA for ACh + ATP, ATP, and ACh, respectively. ***$P < 0.0005$. NS, not significant ($P \geq 0.05$). (C) ATP dose-response curves for P2X3TR oocytes (EC$_{50}$ 9.73 ± 0.29 μM, Hill constant 1.5 ± 0.06, n = 6), P2X3TR–α6β4 oocytes in an absence of ACh (EC$_{50}$ 20.1 ± 5.3 μM, Hill constant 0.97 ± 0.20, n = 7), and P2X3TR–α6β4 oocytes in the presence of 100 μM ACh (EC$_{50}$ 39.0 ± 6.5 μM, Hill constant 1.0 ± 0.13, n = 8). Paralleling the results from full-length P2X3, P2X3TR displayed lower sensitivity toward ATP when α6β4 is coexpressed. (D) Mean, normalized ACh (100 μM), ATP (100 μM), and ATP* currents ± S.E.M. are shown for current signals measured from P2X3TR–α6β4 oocytes (n = 16). Cross inhibition was not observed between P2X3TR and α6β4, in contrast with what was seen with the full-length P2X3 receptor. Mean current amplitudes ± S.E.M. for ACh, ATP, and ATP* are 3.54 ± 0.48 μA, 7.64 ± 0.58 μA, and 7.20 ± 0.64 μA, respectively.

simultaneous application of ACh and αβmeATP (Fig. 6A). Cross-inhibitory behavior was observed from P2X2/3–α6β4 oocytes; the current induced by coapplication of 100 μM αβmeATP and 100 μM ACh ($I_{ACh+αβmeATP}$) was diminished by 19% compared with the predicted value derived from the individual agonist applications (Fig. 6B). Control experiments showed that ACh did not activate or modulate the P2X2/3 receptors in oocytes without α6β4 nAChR (Supplemental

Fig. 5B). Our results indicate a functional interaction between the α6β4 nAChRs and the heteromeric P2X2/3 receptor.

The Role of β3 in Cross Inhibition. As anticipated, only small currents were seen when attempts were made to express wild-type α6β4β3 receptors. Therefore, we introduced a gain-of-function mutation in the β3 subunit, β3(V13′S) (Dash et al., 2011), and this significantly improved expression levels. Once again, we will leave out the V13′S notation for simplicity.
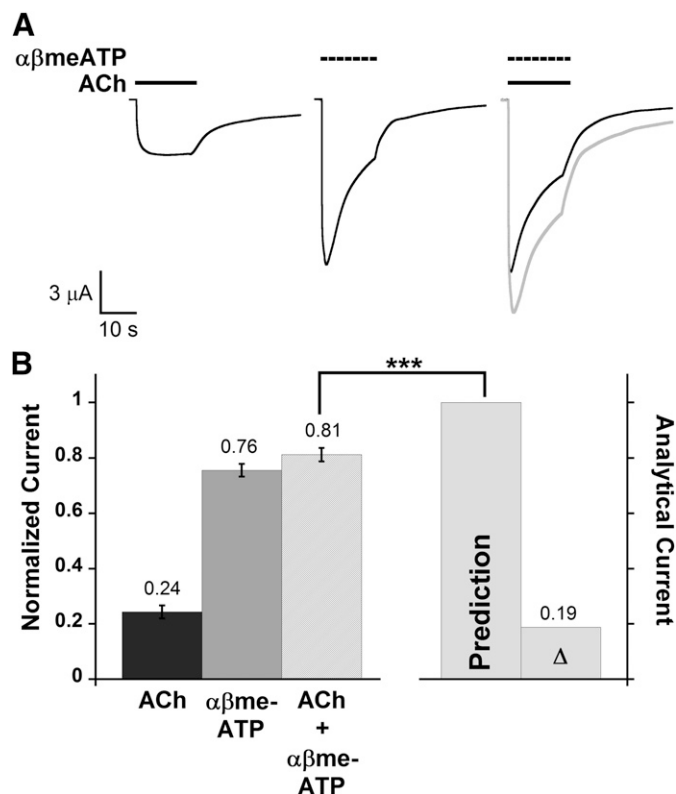
Fig. 6. Functional interaction between the $\alpha6\beta4$ nAChR and the heteromeric P2X2/3 receptor. (A) Representative traces upon application of ACh (100 μM), $\alpha\beta$meATP (100 μM), and ACh + $\alpha\beta$meATP mixture from the same oocyte are shown in black illustrating P2X2/3–$\alpha6\beta4$ cross inhibition. Shown in gray is the predicted waveform, which is the point-by-point arithmetic sum of the I_{ACh} and $I_{\alpha\beta meATP}$ waveforms. (B) Mean normalized agonist-induced currents $\pm$ S.E.M. induced by applying ACh (100 μM), $\alpha\beta$meATP (100 μM), or ACh + $\alpha\beta$meATP to oocytes coexpressing $\alpha6\beta4$ and P2X2/3 receptors (n = 9). All measured current signals were normalized to the predicted arithmetic sum of ACh- and $\alpha\beta$meATP-induced currents ("Prediction" column) of the same cell and then averaged. Mean current amplitudes $\pm$ S.E.M. are 3.25 $\pm$ 0.37 μA for ACh, 10.02 $\pm$ 0.58 μA for $\alpha\beta$meATP, and 10.82 $\pm$ 0.73 μA for ACh + $\alpha\beta$meATP. Δ is the mean difference between the prediction and the observed $I_{ACh+\alpha\beta meATP}$. The paired t test was performed to compare non-normalized $I_{ACh+\alpha\beta meATP}$ data to the predicted values. Cross inhibition was observed from P2X2/3–$\alpha6\beta4$ oocytes, as the observed $I_{ACh+\alpha\beta meATP}$ was significantly smaller than the prediction. ***$P < 0.0005$.

Note that the $\alpha6$ and $\alpha4$ subunits are fully wild type in these studies. Because only a single $\beta3$ subunit is incorporated into nAChR (Drenan et al., 2008b), we assumed the stoichiometry of the $\alpha6\beta4\beta3$ composition to be $(\alpha6)_2(\beta4)_2(\beta3)_1$. A mixed population of nicotinic receptors was not a concern, since wild-type $\alpha6\beta4$ alone produces essentially no current when expressed in oocytes, even when coexpressed with P2X subunits (data not shown).

We found that P2X2–$\alpha6\beta4\beta3$ oocytes exhibited cross inhibition similar to the data for P2X2–$\alpha6\beta4$ oocytes. The total current elicited by a simultaneous application of 100 μM ACh and 1 mM ATP was 19% less than the sum of the current elicited by the individual agonist at the same concentrations (Supplemental Fig. 6A). Likewise, when P2X2TR was coexpressed with $\alpha6\beta4\beta3$, we observed mean $I_{ACh+ATP}$ values that were 23% smaller than the predicted values (Supplemental Fig. 6A), suggesting that the C-terminal tail of P2X2 was not important for the receptor crosstalk.

Functional interaction between $\alpha6\beta4\beta3$ and P2X3 could not be established. First, coexpression of $\alpha6\beta4\beta3$ and P2X3 had a <2-fold effect on the EC$_{50}$ of ACh or ATP, unlike observations for the P2X3–$\alpha6\beta4$ combination (Supplemental Table 1). Second, cross inhibition experiments, performed at 100 μM of both ACh and ATP (saturating concentrations) using the prolonged plus brief pulse protocol, revealed a Δ* value of 0.12 (Supplemental Fig. 6B). This was smaller than the case of P2X3$-\alpha6\beta4$, and a Student's t-test suggested no statistically significant difference between I_{ATP} and I_{ATP*}. Interestingly, when similar cross interaction experiments were performed on P2X2(T18A)$-\alpha6\beta4\beta3$ oocytes, we also observed no clear cross inhibition, because the Δ* value obtained was 0.08 (Supplemental Fig. 6B). Our results, therefore, suggest that the presence of a $\beta3$ subunit weakened the cross inhibition between $\alpha6\beta4$ and the fast-desensitizing P2X receptors, both P2X3 and P2X2(T18A).

The cross-inhibitory behavior was observed when $\alpha6\beta4\beta3$ was coexpressed with P2X2/3. In this case, the current observed when 100 μM ACh and 100 μM $\alpha\beta$meATP were coapplied ($I_{ACh+\alpha\beta meATP}$) was diminished by 17% compared with the predicted value based on the individual agonist applications (Supplemental Fig. 6C).
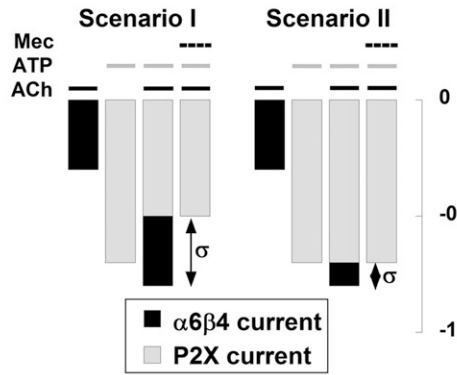
Probing P2X Channel Activity during P2X–$\alpha6\beta4$ Cross Inhibition by Selectively Blocking $\alpha6\beta4$ with Mecamylamine. The cross inhibition between the P2X and the Cys-loop families of ligand-gated ion channels has been postulated to result from a physical occlusion of the ion channel pores during simultaneous agonist application. Investigation of this hypothesis requires an ability to distinguish between the $\alpha6\beta4$ and the P2X ion channel activities. In this study, we used Mec, a selective open channel blocker for several nAChR subtypes, for this purpose.

In oocytes expressing both $\alpha6\beta4$ and P2X receptors, one expects coapplication of Mec, ACh, and ATP to generate inward current ($I_{ACh+ATP+Mec}$), the amplitude of which reflects only the current flowing through P2X channel. This $I_{ACh+ATP+Mec}$ current is not necessarily identical to ATP-evoked current (I_{ATP}) due to the functional interaction between the two families of ligand-gated ion channels. $I_{ACh+ATP+Mec} < I_{ATP}$ implies that the P2X pore was occluded during the cross inhibition (Fig. 7A, scenario I), and $I_{ACh+ATP+Mec} = I_{ATP}$ implies that P2X channel activity was unaffected by the receptor interaction (Fig. 7A, scenario II).

We started by establishing that Mec indeed inhibited $\alpha6\beta4$ ion channel activity. The IC$_{50}$ values were determined to be 9.1 $\pm$ 0.6 μM for $\alpha6\beta4$ and 0.93 $\pm$ 0.13 μM for $\alpha6\beta4\beta3$ oocytes (Supplemental Fig. 7A). In both cases, Mec blockade was reversible and strongly voltage dependent, showing minimal block at positive potentials (Supplemental Fig. 7, B and C). The voltage sensitivity confirms that Mec blocked the receptors in the transmembrane region, simply occluding the channel pore. Hence, the pore blocker is unlikely to interfere with agonist binding, the opening of the pore, or the protein–protein interaction. As anticipated, 500 μM Mec did not affect ATP-evoked current in oocytes expressing P2X2 nor did it affect $\alpha\beta$meATP-evoked current in oocytes expressing P2X2/3.

In P2X2–$\alpha6\beta4$ oocytes, coapplication of ACh, ATP, and Mec produced current ($I_{ACh+ATP+Mec}$) that was significantly smaller than the current induced by ACh + ATP ($I_{ACh+ATP}$) on the same cells (Fig. 7B). In this case, $I_{ACh+ATP+Mec}$ was significantly smaller than I_{ATP}, suggesting that P2X2 was
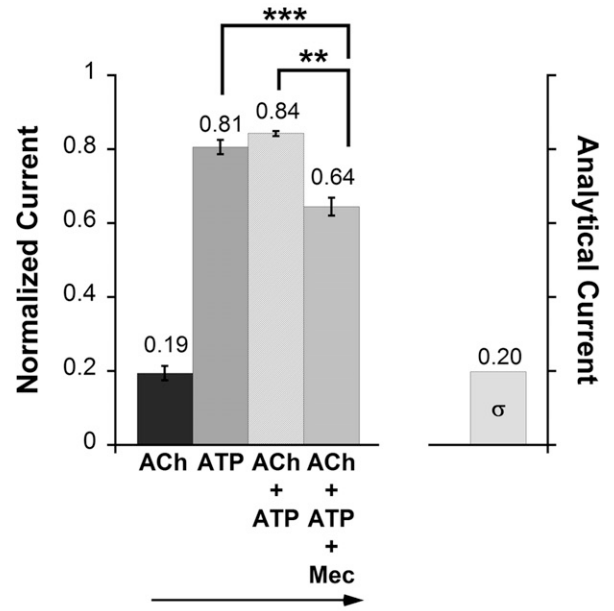
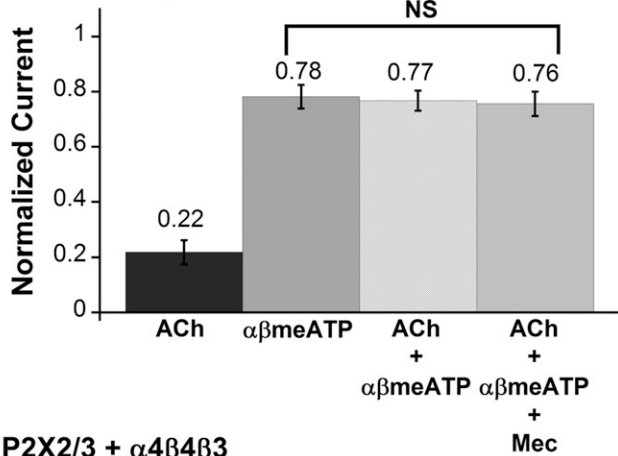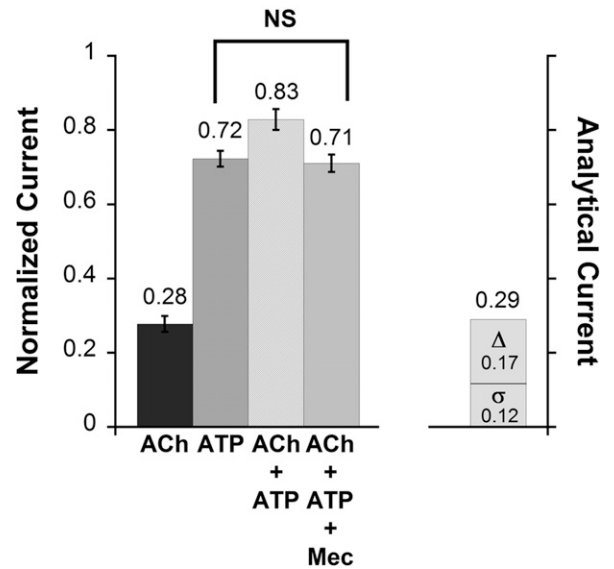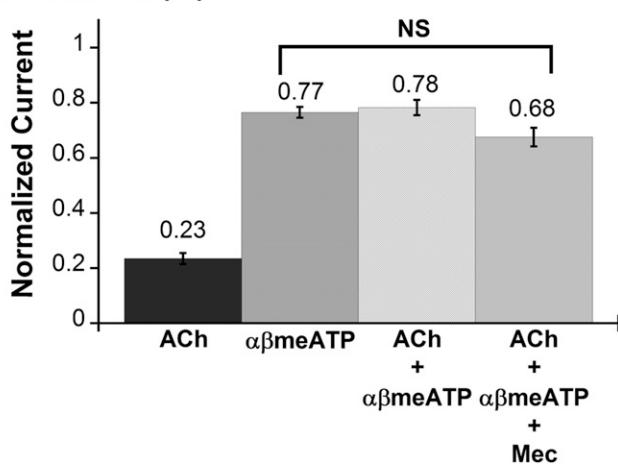**Fig. 7.** Selectively blocking α6β4 channel with Mec reveals P2X channel activity during P2X–α6β4 cross inhibition. (A) Schematic currents illustrate two simple mechanisms underlying P2X–α6β4 cross inhibition. In scenario I, current flowing through P2X (grey bar) is smaller, whereas current flowing through α6β4 (black bar) remains the same during agonist coapplication compared with the current induced by each individual agonist. Scenario II is the opposite of scenario I, in which the same amount of current is flowing through P2X but there is less current through α6β4 during agonist coapplication with respect to during individual agonist application. Mec was used to distinguish between these two possibilities. Coapplying Mec with ACh and ATP results the amount of current flowing through the P2X channel alone when both agonists are present. Therefore, comparison between $I_{ACh+ATP+Mec}$ and I_{ATP} can reveal the underlying mechanism of P2X–α6β4 cross inhibition. (B) Mean normalized currents ± S.E.M. are shown for current signals measured from P2X2–α6β4 oocytes ($n = 8$) in response to ACh (100 µM), ATP (1 mM), ACh + ATP, or ACh + ATP + Mec, in the order indicated by the arrow. Mean current amplitudes ± S.E.M. for ACh, ATP, ACh + ATP, and ACh + ATP + Mec are 2.28 ± 0.34 µA, 9.13 ± 0.38 µA, 9.61 ± 0.56 µA, 7.29 ± 0.36 µA, respectively. σ is the mean difference between $I_{ACh+ATP}$ and $I_{ACh+ATP+Mec}$, indicating the amount of current blocked by Mec. $I_{ACh+ATP+Mec}$ is significantly smaller than I_{ATP}, suggesting that P2X2 channel activity is inhibited during the cross inhibition. σ is essentially identical to I_{ACh}, confirming that α6β4 channel activity was unchanged while the agonists were coapplied. (C) Mean normalized ACh (100 µM), αβmeATP (100 µM), ACh + αβmeATP, and ACh + αβmeATP + Mec currents ± S.E.M. from oocytes coexpressing α6β4 and P2X2/3 receptors ($n = 8$). Mean current amplitudes ± S.E.M. for ACh, αβmeATP, ACh + αβmeATP, and ACh + αβmeATP + Mec are 2.79 ± 0.53 µA, 10.24 ± 1.18 µA, 10.06 ± 1.14 µA, and 9.74 ± 0.96 µA, respectively. Because $I_{ACh+αβmeATP+Mec}$ is approximately equal to $I_{αβmeATP}$, P2X2/3 channel pore was fully active and unaffected by the cross inhibition. (D) Mean normalized currents ± S.E.M. are shown for current signals measured from P2X2–α6β4β3 oocytes ($n = 8$) in response to ACh, ATP, ACh + ATP, or ACh + ATP + Mec. Δ is the mean difference between the prediction and the observed $I_{ACh+ATP}$. σ is the mean difference between $I_{ACh+ATP}$ and $I_{ACh+ATP+Mec}$.

inhibited due to the cross inhibition (Fig. 7A, scenario I). The $\alpha6\beta4$ channel pore was fully functional as the amount of current block by Mec ($I_{ACh+ATP+Mec} - I_{ACh+ATP}$), denoted as σ, was nearly equal to I_{ACh}. Results from control experiments showed no significant difference between the current amplitudes induced by the first and the second ACh + ATP applications (Supplemental Fig. 8). In P2X2/3–$\alpha6\beta4$ oocytes, however, the current elicited by ACh + $\alpha\beta$meATP + Mec ($I_{ACh+\alpha\beta meATP+Mec}$) was essentially identical to $I_{\alpha\beta meATP}$ (Fig. 7C). The data indicate that current flowing through P2X2/3 channel remains the same during the P2X2/3–$\alpha6\beta4$ cross inhibition (Fig. 7A, scenario II).

We observed parallel results from P2X2–$\alpha6\beta4\beta3$ oocytes and P2X2/3–$\alpha6\beta4\beta3$ oocytes, in which $I_{ACh+ATP+Mec}$ is approximately equal to I_{ATP} and $I_{ACh+\alpha\beta meATP+Mec}$ is approximately equal to $I_{\alpha\beta meATP}$, respectively (Fig. 7, D and E). Therefore, both of these cases fall under scenario II of Fig. 7A, in which P2X channels were not altered by the functional interaction with $\alpha6\beta4\beta3$.

Because Mec blockade was generally established with a time constant of a few seconds, these experiments required preincubation with ACh. Therefore, the brief opening lifetime of the fast-desensitizing P2X receptors would not allow for the cross interaction to be probed by Mec.

Overall, our results suggest that the ion channel pores of the P2X receptors were fully functional and unaltered by the cross inhibition in three of four cases that we studied (P2X2–$\alpha6\beta4\beta3$, P2X2/3–$\alpha6\beta4$, and P2X2/3–$\alpha6\beta4\beta3$). The unique exception belongs to P2X2–$\alpha6\beta4$, in which the P2X2 current was reduced during agonist coapplication with Mec. This observation is consistent with our hypothesis that the P2X2 receptor requires a longer time to recover fully from a desensitized state while interacting with $\alpha6\beta4$ nAChR.

Discussion

Previous experiments from several laboratories, summarized in the Introduction, show that the functions of nAChRs and P2X receptors are modulated by each other when they are activated simultaneously by their own neurotransmitters. In this study, we investigated functional interactions between $\alpha6\beta4$ nAChRs and three subtypes of P2X receptors (P2X2, P2X3, and P2X2/3) in *Xenopus* oocytes.

Cross Interactions Involving P2X2. We have established functional interactions between P2X2–$\alpha6\beta4$ in the form of cross inhibition (Fig. 1). We also used the nAChR open channel blocker, Mec, to probe whether P2X current or $\alpha6\beta4$ current was being inhibited. Our data suggest that a fraction of the total P2X2 receptor population was inhibited while most $\alpha6\beta4$ receptors remained fully open (but blocked and therefore nonconducting) during the agonist coapplication (Fig. 7B). We assume that the P2X2 population that was not

inhibited was free of $\alpha6\beta4$ nAChRs because $\alpha6\beta4$ receptors are expressed rather sparsely.

The likely source of the P2X2–$\alpha6\beta4$ cross inhibition is a subpopulation of P2X2 that lingers in a desensitized state after an initial exposure to ATP or ACh + ATP (Fig. 3). The inhibition of current was attributed to desensitization rather than to receptor internalization (Robinson and Murrell-Lagnado, 2013) because current reduction was observed within seconds after agonist coapplication (Supplemental Fig. 3). Therefore, we propose that P2X2–$\alpha6\beta4$ functional interaction could involve prolonged P2X2 desensitized state lifetime(s) in the presence of $\alpha6\beta4$, regardless of the $\alpha6\beta4$ activation by ACh. As usual, when one discusses desensitization, the secondary structures and atomic-scale changes involved remain unclear.

The sequence of agonist application is crucial for the detection of the cross-inhibitory behavior in P2X2–$\alpha6\beta4$ oocytes (Fig. 2; Supplemental Fig. 2) but not in P2X2–$\alpha6\beta4\beta3$ oocytes. The current additivity in Fig. 2, D–F, is quite intriguing. This additivity could mean that the interaction between $\alpha6\beta4$ and P2X2 is uncoupled if both receptors are simultaneously activated. Alternatively, the additivity in Fig. 2, D–F, could indicate that more than one mechanism is at play in P2X2–$\alpha6\beta4$ functional interactions, but their combined effects concealed the overall cross inhibition. For instance, it is possible that a fraction of current was already missing during the ACh + ATP application, through an additional cross-inhibitory mechanism that results in ion pore occlusion, specifically occurring during coactivation of both receptors.

Interestingly, in the presence of $\beta3$, P2X2 that is interacting with $\alpha6\beta4$ seemed to display a usual desensitized state lifetime, even though cross inhibition was still observed (Supplemental Fig. 6A). The results from Mec experiments on P2X2–$\alpha6\beta4\beta3$ oocytes (Fig. 7D) suggest that the ion pore of the P2X2 receptor was fully open, as I_{ATP} is approximately equal to. $I_{ACh+ATP+Mec}$. The fact that I_{ACh} was essentially identical to the sum of Δ and σ strongly indicates that the inhibited channel in the P2X2–$\alpha6\beta4\beta3$ interacting pair is the $\alpha6\beta4\beta3$ channel, unlike the P2X2–$\alpha6\beta4$ interacting pair. Note that in the absence of Mec, two consecutive doses of ACh + ATP produced very similar current sizes (Supplemental Fig. 7). The results highlight the role of the $\beta3$ subunit in the mechanism of P2X2–$\alpha6\beta4$ cross inhibition.

Removal of the P2X2 C-terminal domain did not affect the cross inhibition with $\alpha6\beta4$ or $\alpha6\beta4\beta3$ (Supplemental Fig. 5). Slow recovery from desensitization (>5 minutes) was also observed for the P2X2TR coexpressed with $\alpha6\beta4$ (data not shown). Previous studies on functional interactions between the P2X2 receptor and other pentameric receptors (GABA$_A$, GABA$_C$, 5-HT$_{3A}$, and $\alpha3\beta4$ nAChR) showed that cross inhibition depends the C terminus of P2X2 (Boué-Grabot et al., 2004a; Decker and Galligan, 2010), and cross inhibition was observed only with P2X2 but not with P2X2TR. Our P2X2TR construct is very similar to the construct used in the previous

Mean current amplitudes ± S.E.M. are 2.65 ± 0.29 μA for ACh, 6.89 ± 0.58 μA for ATP, 7.92 ± 0.71 μA for ACh + ATP, and 6.83 ± 0.65 μA for ACh + ATP + Mec. There is no significant difference between $I_{ACh+ATP+Mec}$ and I_{ATP}, suggesting that P2X2 channel activity is unaffected by the cross inhibition. The sum of Δ and σ is roughly equal to total I_{ACh}, implicating inhibition at $\alpha6\beta4\beta3$ channel pore while the agonists were coapplied. (E) Mean normalized currents ± S.E.M. from oocytes coexpressing $\alpha6\beta4\beta3$ and P2X2/3 receptors ($n = 8$). Mean current amplitudes ± S.E.M. for ACh, $\alpha\beta$meATP, ACh + $\alpha\beta$meATP, and ACh + $\alpha\beta$meATP + Mec are 2.77 ± 0.25 μA, 9.23 ± 0.73 μA, 9.36 ± 0.68 μA, and 8.07 ± 0.67 μA, respectively. The difference between $I_{ACh+\alpha\beta meATP+Mec}$ and $I_{\alpha\beta meATP}$ is not statistically significant; therefore, the P2X2/3 channel activity is likely unchanged during the agonist coapplication. $**P < 0.005$; $***P < 0.0005$. NS, not significant ($P \geq 0.05$).

work, but our result differs, indicating that the underlying mechanism of interaction between P2X2 and α6β4 is unique. While this article was in preparation, another group identified two amino acids downstream of the P2X2 second transmembrane region that regulate recovery from desensitization (Hausmann et al., 2014). These amino acids are between the P2X2 second transmembrane region pore-forming sequence and the C-terminal of P2X2TR translation; possibly this is a region where P2X2 makes molecular contact with α6β4.

Nevertheless, our results suggest that 1) cross inhibition between P2X2 and α6β4 receptors resulted from prolonged desensitization of the P2X2 receptor, 2) the desensitized P2X2 receptor can no longer interact with the α6β4 receptor, 3) additional cross-inhibitory behavior also take place while ACh and ATP are coapplied, and 4) the C-terminal tail of P2X2 (from Pro373 onward) is not necessary for P2X2–α6β4 cross inhibition. Other investigators have seen different roles for desensitization for different receptor combinations (Nakazawa, 1994; Khakh et al., 2000; Decker and Galligan, 2009), indicating that the detailed cross-inhibitory mechanism varies within the P2X and Cys-loop receptor subtypes involved in the interaction.

Cross Interactions Involving P2X3. Because the homomeric P2X3 receptor opens and desensitizes several fold more rapidly than α6β4, we developed the prolonged plus brief pulse protocol to probe their interaction. Two lines of evidence support a P2X3–α6β4 functional interaction. First, cross inhibition was observed between α6β4 and P2X3 receptors (Fig. 4A). In this case, the distinctive waveform of the P2X3 response allows the direct observation that a fraction of current was inhibited as ATP was applied in the presence of ACh, versus the response to ATP applied alone (Fig. 4A, inset). Second, oocytes coexpressing α6β4 and P2X3 also exhibited lower ATP sensitivity compared with the oocytes expressing P2X3 alone, independent of α6β4 activation by ACh (Fig. 4B). However, when the C terminus of P2X3 was truncated, cross inhibition was no longer observed (Fig. 5D), although the ATP dose-response relation was still shifted to the right (Fig. 6C). The rightward shift in the ATP dose-response curve seen for the P2X3–α6β4 interaction is specific for this particular pair of receptors, as the effect was not seen with P2X2(T18A). The results altogether suggest two distinct modes of cross inhibition between P2X3 receptors and α6β4: 1) a decrease in the maximal I_{ATP} response, which requires the C-terminal domain of P2X3; and 2) a decrease in ATP sensitivity, which is independent of the C-terminal domain. β3 nAChR had clearly weaker interactions than α6β4 with P2X3 (Supplemental Fig. 6B).

Cross Interactions Involving P2X2/3. We probed the P2X2/3–α6β4 interaction utilizing the simple simultaneous application protocol (Fig. 6A). Cross inhibition was observed in both P2X2/3–α6β4 (Fig. 6B) and P2X2/3–α6β4β3 oocytes (Supplemental Fig. 6C), independent of the order of agonist application. In addition, the two cell types produced comparable results in the experiments with Mec—there was no significant difference between $I_{ACh+αβmeATP+Mec}$ and $I_{αβmeATP}$ (Fig. 7, C and E). Our results demonstrate that current flowing through P2X2/3 was unaffected by the interaction with α6β4*. The reciprocal experiment, with a specific P2X2/3 open channel blocker, is required to show whether the nAChRs were inhibited. Although detailed analysis of functional interactions of α6β4* nAChRs with P2X2/3 is highly desired,

it is inevitably complicated by mixtures of several receptor populations in the cells, including free P2X2, α6β4-bound P2X2, P2X3, α6β4-bound P2X3, free P2X2/3, α6β4-bound P2X2/3, and free α6β4. For instance, comparison between I_{ACh} and σ, as we did for P2X2 interaction, is not meaningful in the case of P2X2/3 because I_{ACh} is a composite current arising from all of the subpopulations in the cell that contain nAChR.

Implications for Neuronal Function. All of the α6β4* nAChRs and P2X2, P2X3, and P2X2/3 receptors studied here are expressed in DRG neurons (Cockayne et al., 2000, 2005; Souslova et al., 2000; Hone et al., 2011; Beggs et al., 2012), although it is not yet known whether individual DRG neurons coexpress them. In addition, in DRG neurons, acid-sensing ion channels appear to interact functionally with another member of the P2X receptor family (Birdsong et al., 2010).

Our results reveal two distinct types of interaction. The first type is dynamic and takes the form of current inhibition, happening only when both receptors are activated. That is, when ACh and ATP are both applied, the agonist-induced currents are less than the sum of individual currents. This type of mechanism is commonly observed between Cys-loop receptors and P2X receptors (see the *Introduction*). The second type of interaction is preorganized—a biophysical property of one channel is allosterically modulated by the other. This type of interaction includes a change in P2X2 desensitization properties in the presence of α6β4 and a shift in P2X3 EC$_{50}$. This type of cross inhibition was previously reported for the P2X2–α3β4 nAChR pair, in the form of constitutive current suppression and a shift in the dose-response relation (Decker and Galligan, 2010). This functional crosstalk between two families of ligand-gated ion channels may play an important role in communication between neurons, by an efficient way to adapt neurotransmitter signaling to fluctuating functional needs on the subsecond and second time scales. It will take some time to describe the molecular details of these diverse interactions, but this work elucidates a more detailed mechanism and specificity of functional interaction between specific pairs of α6β4* nAChRs and P2X receptors.

Authorship Contributions

Participated in research design: Limapichat, Dougherty, Lester.
Conducted experiments: Limapichat.
Performed data analysis: Limapichat, Dougherty, Lester.
Wrote or contributed to the writing of the manuscript: Limapichat, Dougherty, Lester.

References

Beggs S, Trang T, and Salter MW (2012) P2X4R+ microglia drive neuropathic pain. *Nat Neurosci* 15:1068–1073.

Birdsong WT, Fierro L, Williams FG, Spelta V, Naves LA, Knowles M, Marsh-Haffner J, Adelman JP, Almers W, and Elde RP et al. (2010) Sensing muscle ischemia: coincident detection of acid and ATP via interplay of two ion channels. *Neuron* 68:739–749.

Boué-Grabot E, Barajas-López C, Chakfe Y, Blais D, Bélanger D, Emerit MB, and Séguéla P (2003) Intracellular cross talk and physical interaction between two classes of neurotransmitter-gated channels. *J Neurosci* 23:1246–1253.

Boué-Grabot E, Emerit MB, Toulmé E, Séguéla P, and Garret M (2004a) Cross-talk and co-trafficking between ρ1/GABA receptors and ATP-gated channels. *J Biol Chem* 279:6967–6975.

Boué-Grabot E, Toulmé E, Emerit MB, and Garret M (2004b) Subunit-specific coupling between γ-aminobutyric acid type A and P2X2 receptor channels. *J Biol Chem* 279:52517–52525.

Bray D and Duke T (2004) Conformational spread: the propagation of allosteric states in large multiprotein complexes. *Annu Rev Biophys Biomol Struct* 33:53–73.

Cockayne DA, Dunn PM, Zhong Y, Rong W, Hamilton SG, Knight GE, Ruan HZ, Ma B, Yip P, and Nunn P et al. (2005) P2X2 knockout mice and P2X2/P2X3 double knockout mice reveal a role for the P2X2 receptor subunit in mediating multiple sensory effects of ATP. *J Physiol* **567**:621–639.

Cockayne DA, Hamilton SG, Zhu QM, Dunn PM, Zhong Y, Novakovic S, Malmberg AB, Cain G, Berson A, and Kassotakis L et al. (2000) Urinary bladder hyporeflexia and reduced pain-related behaviour in P2X3-deficient mice. *Nature* **407**:1011–1015.

Dash B, Bhakta M, Chang Y, and Lukas RJ (2011) Identification of N-terminal extracellular domain determinants in nicotinic acetylcholine receptor (nAChR) α6 subunits that influence effects of wild-type or mutant β3 subunits on function of α6β2*- or α6β4*-nAChR. *J Biol Chem* **286**:37976–37989.

Dash B and Lukas RJ (2012) Modulation of gain-of-function α6*-nicotinic acetylcholine receptor by β3 subunits. *J Biol Chem* **287**:14259–14269.

Decker DA and Galligan JJ (2009) Cross-inhibition between nicotinic acetylcholine receptors and P2X receptors in myenteric neurons and HEK-293 cells. *Am J Physiol Gastrointest Liver Physiol* **296**:G1267–G1276.

Decker DA and Galligan JJ (2010) Molecular mechanisms of cross-inhibition between nicotinic acetylcholine receptors and P2X receptors in myenteric neurons and HEK-293 cells. *Neurogastroenterol Motil* **22**:901–908, e235.

Drenan RM, Grady SR, Whiteaker P, McClure-Begley T, McKinney S, Miwa JM, Bupp S, Heintz N, McIntosh JM, and Bencherif M et al. (2008a) In vivo activation of midbrain dopamine neurons via sensitized, high-affinity α 6 nicotinic acetylcholine receptors. *Neuron* **60**:123–136.

Drenan RM, Nashmi R, Imoukhuede P, Just H, McKinney S, and Lester HA (2008b) Subcellular trafficking, pentameric assembly, and subunit stoichiometry of neuronal nicotinic acetylcholine receptors containing fluorescently labeled α6 and β3 subunits. *Mol Pharmacol* **73**:27–41.

Egan TM, Samways DS, and Li Z (2006) Biophysics of P2X receptors. *Pflugers Arch* **452**:501–512.

Eickhorst AN, Berson A, Cockayne D, Lester HA, and Khakh BS (2002) Control of P2X(2) channel permeability by the cytosolic domain. *J Gen Physiol* **120**:119–131.

Fujiwara Y and Kubo Y (2004) Density-dependent changes of the pore properties of the P2X2 receptor channel. *J Physiol* **558**:31–43.

Grinevich VP, Letchworth SR, Lindenberger KA, Menager J, Mary V, Sadieva KA, Buhlman LM, Bohme GA, Pradier L, and Benavides J et al. (2005) Heterologous expression of human α6β4β3α5 nicotinic acetylcholine receptors: binding properties consistent with their natural expression require quaternary subunit assembly including the α5 subunit. *J Pharmacol Exp Ther* **312**:619–626.

Hausmann R, Bahrenberg G, Kuhlmann D, Schumacher M, Braam U, Bieler D, Schlusche I, and Schmalzing G (2014) A hydrophobic residue in position 15 of the rP2X3 receptor slows desensitization and reveals properties beneficial for pharmacological analysis and high-throughput screening. *Neuropharmacology* **79**:603–615.

Hone AJ, Meyer EL, McIntyre M, and McIntosh JM (2011) Nicotinic acetylcholine receptors in dorsal root ganglion neurons include the α6β4* subtype. *FASEB J* **26**:917–926.

Jarvis MF and Khakh BS (2009) ATP-gated P2X cation-channels. *Neuropharmacology* **56**:208–215.

Jensen AB, Hoestgaard-Jensen K, and Jensen AA (2013) Elucidation of molecular impediments in the α6 subunit for in vitro expression of functional α6β4* nicotinic acetylcholine receptors. *J Biol Chem* **288**:33708–33721.

Jo YH, Donier E, Martinez A, Garret M, Toulmé E, and Boué-Grabot E (2011) Cross-talk between P2X4 and γ-aminobutyric acid, type A receptors determines synaptic efficacy at a central synapse. *J Biol Chem* **286**:19993–20004.

Khakh BS, Fisher JA, Nashmi R, Bowser DN, and Lester HA (2005) An angstrom scale interaction between plasma membrane ATP-gated P2X2 and alpha4beta2 nicotinic channels measured with fluorescence resonance energy transfer and total internal reflection fluorescence microscopy. *J Neurosci* **25**:6911–6920.

Khakh BS, Zhou X, Sydes J, Galligan JJ, and Lester HA (2000) State-dependent cross-inhibition between transmitter-gated cation channels. *Nature* **406**:405–410.

Nakazawa K (1994) ATP-activated current and its interaction with acetylcholine-activated current in rat sympathetic neurons. *J Neurosci* **14**:740–750.

Pratt EB, Brink TS, Bergson P, Voigt MM, and Cook SP (2005) Use-dependent inhibition of P2X3 receptors by nanomolar agonist. *J Neurosci* **25**:7359–7365.

Robinson LE and Murrell-Lagnado RD (2013) The trafficking and targeting of P2X receptors. *Front Cell Neurosci* **7**:233.

Searl TJ, Redman RS, and Silinsky EM (1998) Mutual occlusion of P2X ATP receptors and nicotinic receptors on sympathetic neurons of the guinea-pig. *J Physiol* **510**:783–791.

Shrivastava AN, Triller A, Sieghart W, and Sarto-Jackson I (2011) Regulation of GABA(A) receptor dynamics by interaction with purinergic P2X(2) receptors. *J Biol Chem* **286**:14455–14468.

Silinsky EM (1975) On the association between transmitter secretion and the release of adenine nucleotides from mammalian motor nerve terminals. *J Physiol* **247**:145–162.

Silinsky EM and Hubbard JI (1973) Biological sciences: Release of ATP from rat motor nerve terminals. *Nature* **243**:404–405.

Souslova V, Cesare P, Ding Y, Akopian AN, Stanfa L, Suzuki R, Carpenter K, Dickenson A, Boyce S, and Hill R et al. (2000) Warm-coding deficits and aberrant inflammatory pain in mice lacking P2X3 receptors. *Nature* **407**:1015–1017.

Toulmé E, Blais D, Léger C, Landry M, Garret M, Séguéla P, and Boué-Grabot E (2007) An intracellular motif of P2X(3) receptors is required for functional cross-talk with GABA(A) receptors in nociceptive DRG neurons. *J Neurochem* **102**:1357–1368.

Tumkosit P, Kuryatov A, Luo J, and Lindstrom J (2006) β3 subunits promote expression and nicotine-induced up-regulation of human nicotinic α6* nicotinic acetylcholine receptors expressed in transfected cell lines. *Mol Pharmacol* **70**:1358–1368.

Vial C, Roberts JA, and Evans RJ (2004) Molecular properties of ATP-gated P2X receptor ion channels. *Trends Pharmacol Sci* **25**:487–493.

Xia R, Mei ZZ, Milligan C, and Jiang LH (2008) Inhibitory interaction between P2X4 and GABA(C) ρ1 receptors. *Biochem Biophys Res Commun* **375**:38–43.

Zhou X and Galligan JJ (1998) Non-additive interaction between nicotinic cholinergic and P2X purine receptors in guinea-pig enteric neurons in culture. *J Physiol* **513**:685–697.

Address correspondence to: Henry A. Lester, Division of Biology and Biological Engineering, California Institute of Technology, 1200 E. California Blvd., Pasadena, CA 91125. E-mail: lester@caltech.edu